

Confocal Raman & AFM Imaging of Paper

Introduction

Papermaking has a 2000-year-long manufacturing history that launched a revolution in communication, packaging, and personal care products. Over the centuries, paper has made a great contribution to civilization and still contributes to the rapid advancement of every other industry. Paper is produced by pressing together moist plant fibers, typically cellulose pulp derived from wood, rags or grasses and drying them into flexible sheets. These fibers are composed of cellulose, hemicelluloses, lignin and small quantities of extractives.

The properties of paper are determined primarily by the cellulose fiber composition. Most papers are then further processed by various chemical treatments including bleaching and lamination. A detailed understanding of the micro- and nanostructures of the paper in its successive stages of production as well as the final paper composition at a sub-micron level are essential for further improvement of its properties. With

the advancement of nano-analytical instrumentation this detailed knowledge has become readily accessible.

Confocal Raman imaging is a valuable tool for such studies, as it not only reveals optical information but also information regarding the 3D distribution of the chemical compounds in the submicrometer range [1-3]. In the paper surface finishing process additional surface roughness parameters can be measured by combining the confocal Raman microscope with an atomic force microscope (AFM). Such combined analytical microscopes allow a direct linking between high resolution imaging and chemical identification of various chemical compounds on a surface.

The aim of this application note is to present examples of confocal Raman and AFM measurements from several stages of the paper manufacturing process followed by examples where such measurements give more insight into printing and writing on paper.

Experimental Methods

All experiments were performed with the confocal Raman microscopes of the alpha300 R or alpha500 R series, whereas combined Raman and AFM measurements were performed with an alpha300 RA microscope. The alpha300 microscope series is optimized for high resolution imaging of samples and is able to combine several analytical measuring techniques in one instrument such as: diffraction-limited confocal microscopy, chemically-sensitive Raman spectroscopy and cantilever based scanning probe microscopy, including AFM and SNOM. Using these instruments it is possible to analyze the same sample position with various measuring techniques sequentially or even in parallel (Raman and AFM). The alpha300 R Plus and the alpha500 microscope series add automation and large scan area measuring capabilities. The confocal Raman microscope can be equipped with a variety of excitation lasers. For the measurements presented in this application note, either a frequency-

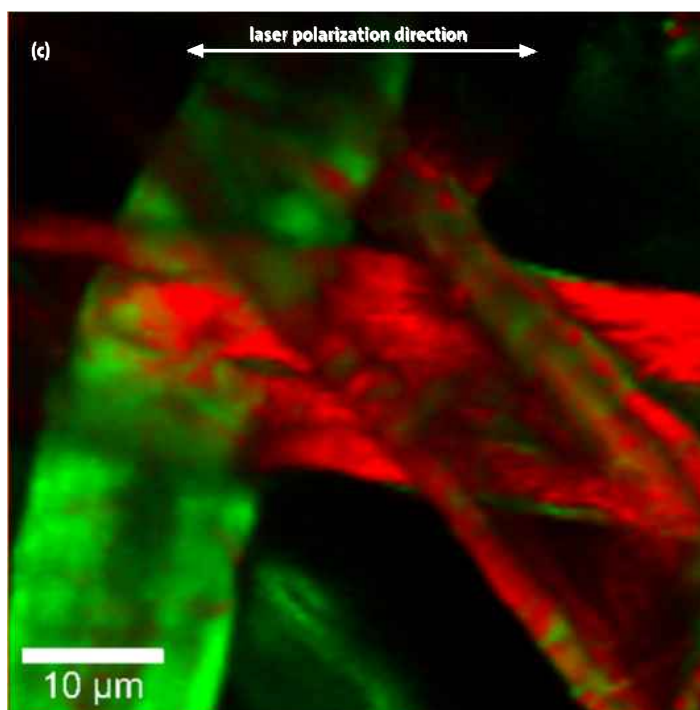
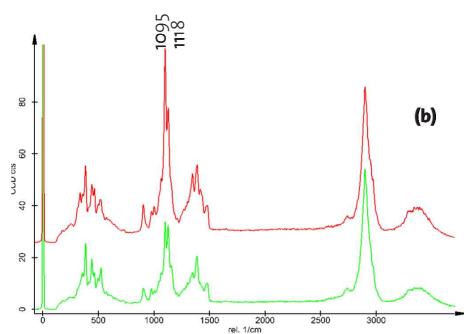
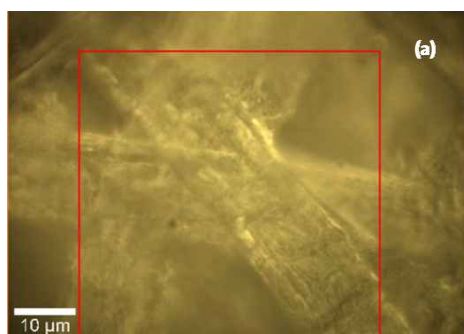


Fig. 1: Confocal Raman imaging of raw cellulose fiber bundles. Video image (a), orientation-dependent Raman spectra of cellulose (b) and color-coded Raman image of cellulose fibers (c). Image area 50x50 μm², 128x128 pixels, integration time: 80 ms/spectrum.

doubled NdYAG laser: $\lambda = 532 \text{ nm}$ (in the following called green laser) or a diode laser: $\lambda = 785 \text{ nm}$ (in the following called NIR laser) were used. The excitation light was polarized horizontally (in the x-direction) with respect to the Raman image. All measurements were performed using an UHTS300 (ultra-high-throughput spectrometer) and back-illuminated CCD cameras.

The distribution of chemical species on the sample was obtained in Raman spectral imaging mode. In this imaging mode a complete Raman spectrum is recorded at every imaging point, leading to a 2D array of Raman spectra. By extracting individual features such as Raman peak intensity, peak width or peak position from the recorded 2D arrays of

spectra, Raman images can be calculated displaying a variety of information contents. Furthermore, fitting algorithms can be employed to extract additional images from the recorded 2D arrays of Raman spectra [4]. The combination of such images allow the illustration of the distribution of various compounds in one image. The illustration colors are coded in the same way for the corresponding spectra. The acquisition time for a Raman spectrum within a 2D spectral array was only a few milliseconds or 10s of milliseconds, thus allowing the acquisition of thousands of Raman spectra within minutes. The number of pixels and the integration times per spectrum are listed in the sections describing the corresponding Raman image throughout this document.

By rotating the microscope turret, it is possible to switch between confocal Raman microscopy and AFM without losing the sample position. The samples were imaged in AFM AC Mode using ArrowFM cantilevers (Nanoworld, Germany) with a resonance frequency in the range of 70–90 kHz and damping of $r = 50\%$, recording both topography and phase images simultaneously.

Paper production

Depending on the scope of use, paper has to meet multiple requirements, consequentially leading to a variety of production methods. For the production of packaging paper with short fiber lengths and a yellowish color, a mechanical pulping is sufficient. In this process lignin is not removed from the pulp, leading

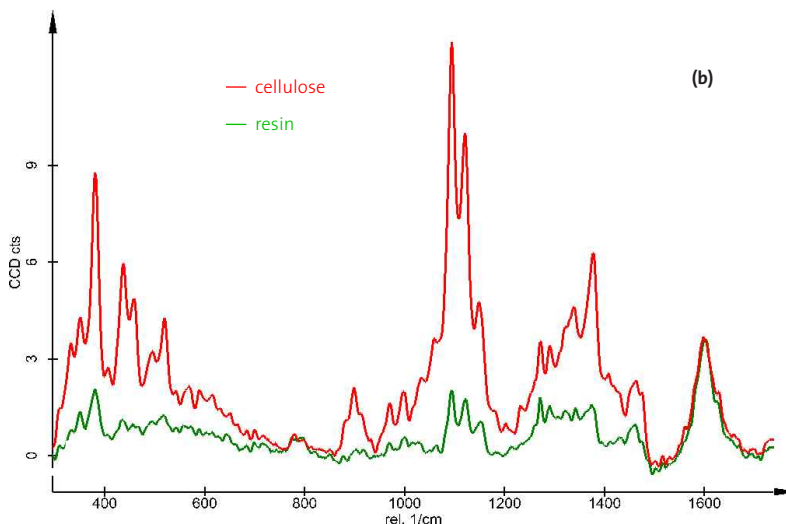
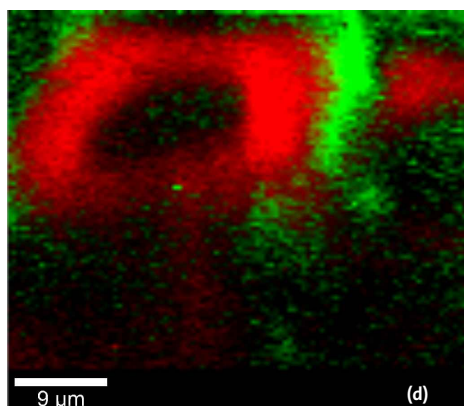
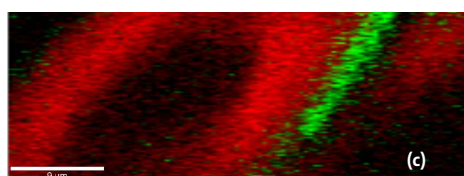


Fig. 2: Confocal Raman study of resin distribution around cellulose fibers. Video image (a), Raman spectra of resin (green) and cellulose (red) (b), color-coded Raman image of a surface scan, image area $45 \times 17 \mu\text{m}^2$, 100×100 pixels, integration time: 112 ms/spectrum. (c), and a depth profile (d). Image area $45 \times 40 \mu\text{m}^2$, 100×100 pixels, integration time: 112 ms/spectrum.

to a high production yield. High quality paper for writing and printing requires chemical pulping. In this process the chemical structure of lignin is destroyed and dissolved in the pulp and can be washed off the cellulose fibers. Furthermore, the fiber length is preserved leading to stronger paper. The finished paper is then produced by feeding the pulp into a paper machine where it is formed as a paper web and the water is removed from the paper by pressing and drying. In the following, the spectral differences of pure cellulose are first illustrated then followed by the analysis of residues on cellulose fibers

Raman imaging of a pure cellulose paper web

Fig. 1a shows the video image of a paper web consisting of pure cellulose fibers. The red square in this video image indicates the area scanned in Raman spectral imaging mode using green excitation and a high numerical aperture air objective. An area of $50 \times 50 \mu\text{m}^2$ was scanned and a 2D spectral array of 128×128 complete Raman spectra was recorded with an integration time of 80 ms/spectrum. From this 2D array of spectra, two distinct spectra for cellulose were extracted which are shown in Fig. 1 b. The assignment of the various Raman bands characteristic for cellulose can be found in [4]. A significant difference between the two spectra can be seen in the intensity variation of the Raman bands at $1095/\text{cm}$ and $1118/\text{cm}$. These two bands are characteristic for C-O and C-C stretching, respectively, and are laser polarization direction dependent. The distribution of these two Raman spectra over the examined surface area is presented in Fig. 1c. The color of the spectra in Fig. 1b matches the color in the Raman image. Thus, pixels which are bright green show a high spectral similarity to the green spectrum, whereas bright red pixels show a high spectral similarity to the red spectrum. The laser polarization direction is indicated with the white arrow in Fig. 1c. Fibers oriented parallel to the laser polarization direction show an increased C-O stretching band at $1095/\text{cm}$ (red color) compared to fibers oriented perpendicular to the laser

polarization direction (green color). Thus, confocal Raman microscopy easily reveals the orientation of cellulose fibers in the paper web even when not determined microscopically.

Raman and AFM imaging of residues on cellulose fibers

As mentioned before, lignin is washed off the cellulose fibers during the chemical pulping. Furthermore, the small quantities of extractives such as resin acids, triglycerides, steryl esters, fatty acids, sterols, and lignins can be extracted from wood by using solvents such as acetone or dichloromethane. During the papermaking process, these extractives are partly released into the circulation water. Today, efforts are made to decrease the water consumption in paper mills. Hence, water is re-circulated in the process, which leads to a build-up of dissolved and colloidal substances. The enrichment of extractives in the circulating water in particular leads to problems such as precipitates, paper strength decreases and foaming. The following two examples show studies of residues and their distribution on cellulose fibers.

Fig. 2 shows an example of a study of resin distribution in paper. For this experiment a sheet of paper was soaked in water to reduce the strong fluorescence of the sample. The alpha300R was equipped with a NIR excitation laser and a back-illuminated deep depletion CCD camera. A water immersion objective (NA = 1.0) was used for these measurements. The video image in Fig. 2a shows several cellulose fibers oriented almost perpendicular to the polarization direction of the laser. The red square denotes the in-plane (x-y) scanned area of $45 \times 17 \mu\text{m}^2$. The blue line indicates where the depth (x-z) scan was performed. For the in-plane scan an array of 100×100 Raman spectra was recorded with an integration time of 0.112 s/spectrum. Fig. 2b shows the characteristic Raman spectra extracted from the spectral array. The distribution of cellulose (red) and resin (green) on the analyzed sample area is shown in Fig. 2c. This image shows that

the resin is distributed between the analyzed fibers. Fig. 2d shows a depth (x-z) scan of the sample. In this case an array of 100×100 Raman spectra was recorded over a range of $45 \times 40 \mu\text{m}^2$. The color-coded image presented in Fig. 2d clearly shows that the resin is surrounds the cellulose fiber, without penetrating into it.

A further survey was performed using the combination of confocal Raman and AFM to detect traces of wood extractives on pure cellulose fibers. An area of $20 \times 40 \mu\text{m}^2$ was scanned in Raman spectral imaging mode by acquiring a spectral array of 80×160 complete Raman spectra. From this spectral array three distinct spectra were extracted as shown in

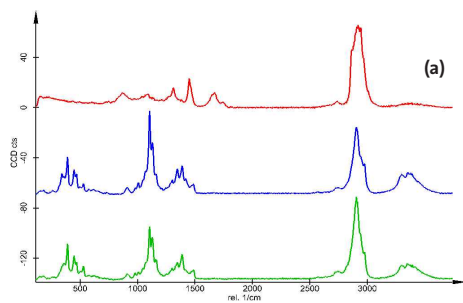


Fig. 3a. The green and blue spectra are the orientation-dependent Raman spectra of cellulose, whereas the red spectrum represents hexane-extractives, forming a very thin layer on the cellulose fibers [4]. The distribution of these three chemical compounds on the analyzed sample area is shown in the color-coded Raman image (Fig. 3b). The white rectangle in Fig. 3b marks the area which was imaged in AFM AC mode. Fig. 3c shows the topography image of a fiber bundle consisting of small, oriented fibrills, characteristic for cellulose fibers. The simultaneously recorded phase image (Fig. 3d) reveals in the central part an additional contrast which can be attributed to the hexane extractive. High-resolution AFM AC images recorded from this region are shown in Figs. 3e (topography

image) and 3f (phase image). The hexane extractives show a clear contrast in the phase image, revealing a material with different mechanical properties than the cellulose fibrills underneath.

Further details on the morphological and structural changes associated with mercerization of cellulose fibers are presented in [5].

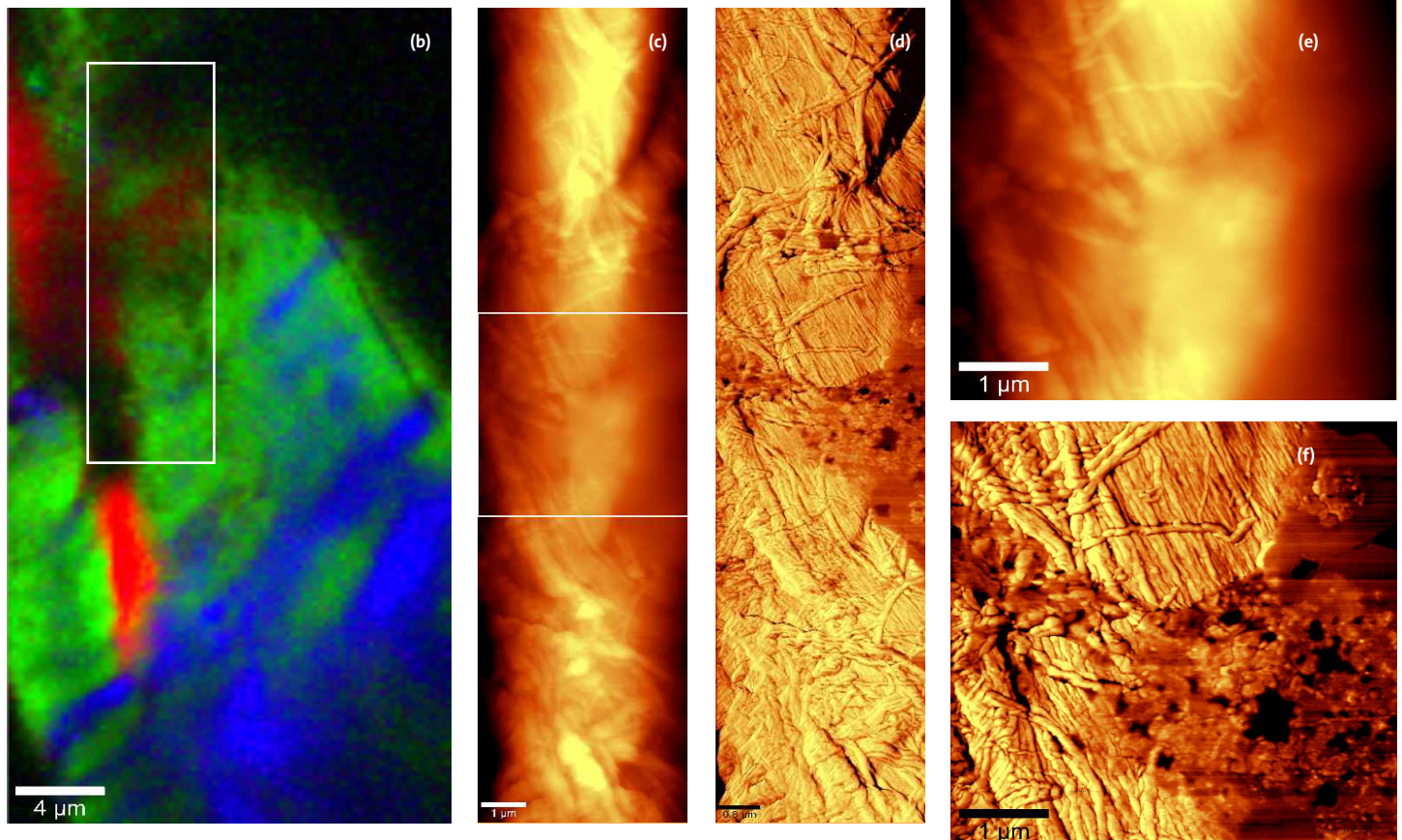


Fig. 3: Confocal Raman AFM images of traces of wood extractives on cellulose fibers: Raman spectra of cellulose (green and blue spectrum) and hexane extract (red spectrum) (a), color-coded Raman image of a cellulose fiber) image area $20 \times 40 \mu\text{m}^2$, 80×160 pixels, integration time: 100 ms/spectrum. (b), high-resolution AFM topography (c, e) and phase image (d, f) of the fiber. Zoomed AFM AC images (e, f).

Paper Finishing

The pure cellulose paper introduced in the previous section is a yellowish, rough paper, which can hardly be used for writing and printing. To provide a surface more suitable for high-resolution halftone screening, the raw paper is coated with a thin layer of calcium carbonate and other additives. Confocal Raman imaging and AFM can provide valuable information on their distribution and effect as the following examples will illustrate.

Fig. 4 shows the distribution of calcium carbonate on coated paper. This image was obtained with the green laser and a 40x air objective (NA = 0.6). An area of 150x150 μm^2 was scanned in Raman spectral imaging mode and an array of 150x150 Raman spectra was

recorded with an integration time of 0.09 s/spectrum. Red and green in Fig. 4 denote the different orientation of the cellulose fibers, whereas blue shows the distribution of calcite on the paper.

Fig. 5 shows additional additives in the paper coating. These additives lead to a higher halftone screen of the paper surface. The coating of this sample contains besides calcite (blue color) also starch grains (red color) and a polymeric matrix (green color). The cellulose is shown in yellow color in this image without specific labeling of the fiber orientation.

AFM can additionally contribute to the analysis of paper finishing with high-resolution images that describe the surface

roughness of the paper (Fig. 6). The topography of raw paper is shown in Fig. 6a, revealing the fibrillar fine structure of cellulose fibers with diameters in the nm-range. This surface is rather rough and can not be used for writing or printing. In Fig. 6b and 6c the topography of laminated paper is shown after applying one and two laminations, respectively. The roughness parameters calculated from these differently processed paper surfaces using the WITec Project data analysis tools [6] are summarized in table 1. From these results it is evident that at least two layers of lamination should be applied in order to decrease the surface roughness. The combined Raman-AFM studies give insight into the chemical nature of the additives and laminates as well as their effect on the surface roughness.

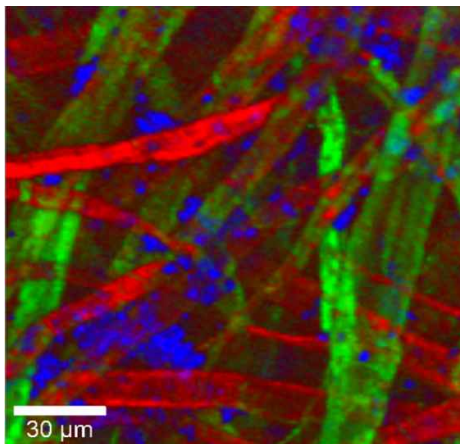


Fig. 4: The distribution of calcite (blue) on cellulose paper (red and green color show the different orientations of the cellulose fibers), image area 150x150 μm^2 , 150x150 pixels, integration time: 90 ms/spectrum.

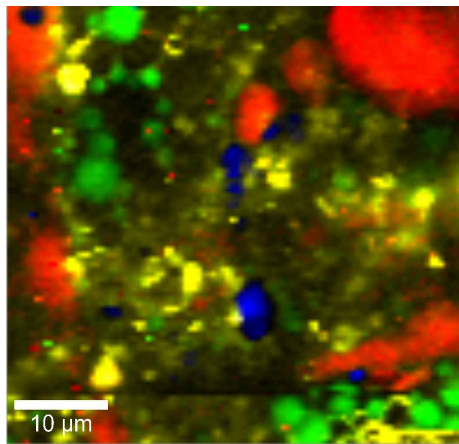


Fig. 5: The distribution of starch (red), calcite (blue) and a polymeric material (green) on cellulose paper (yellow), image area 50x50 μm^2 , 100x100 pixels, integration time: 512 ms/spectrum.

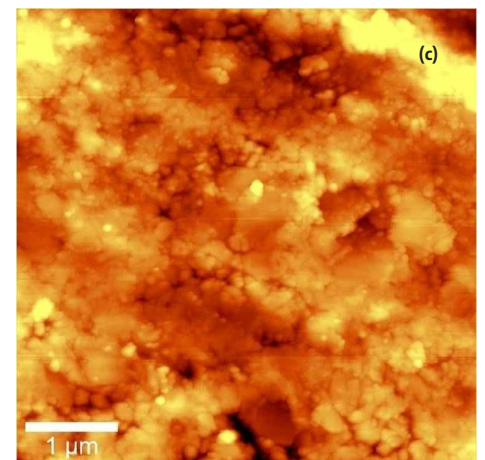
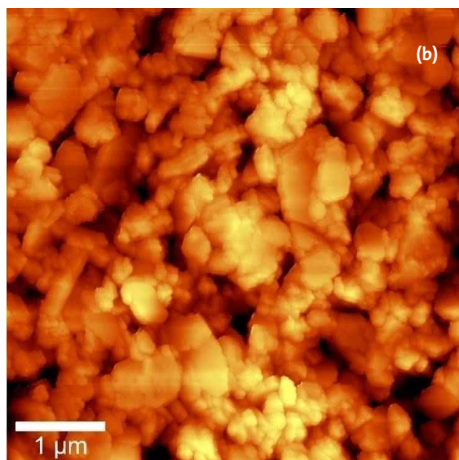
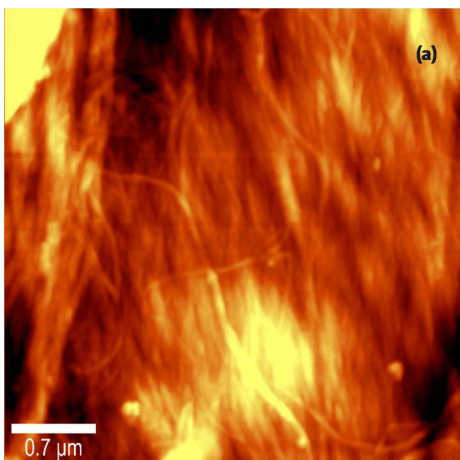


Fig. 6: High-resolution AFM images of untreated paper (a) and laminated paper after applying one layer (b) and two layers (c).

	raw paper	one layer	two layer
Analyzed area	27 μm^2	27 μm^2	25 μm^2
True area	29 μm^2	34 μm^2	26 μm^2
Peak-peak	378 nm	494 nm	194 nm
Roughness surface average (SA)	35 nm	39 nm	12 nm
Roughness mean square (SQ)	47 nm	50 nm	16 nm

Table 1: Roughness parameters

Paper Coating

Depending on the final application of the paper, its composition can consist of several different layers. Confocal Raman imaging can contribute to the analysis of paper layers in a nondestructive way. Fig. 7 shows a depth scan (x-z scan) obtained from a multi-colored paper. An area of $60 \times 100 \mu\text{m}^2$ was scanned in the x-z plane and an array of 100×250 Raman spectra was recorded with an integration time of 50 ms/spectrum. This experiment was performed using the green excitation laser and an oil immersion objective (NA = 1.25). The distribution of the various color-coded materials can be clearly seen in Fig. 7, while the chemical composition of the various materials need to remain undisclosed due to confidentiality. The image clearly reveals the presence of 10 different layers along a depth of $100 \mu\text{m}$. Most of the coatings used form a well defined interface without penetrating into one another.

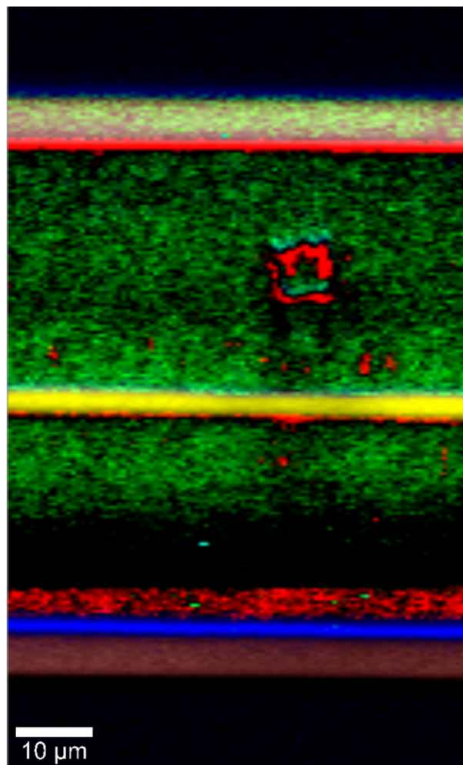


Fig. 7: Depth scan through a multilayer coating of a paper sample. Different colors in the image represent different coating materials. Image area $60 \times 100 \mu\text{m}^2$, 100×250 pixels, integration time: 50 ms/spectrum.

Another example of a modified paper is shown in Fig. 8. In this case two adhesives were applied to the paper surface to produce a sticky paper label. In this experiment an area of $50 \times 40 \mu\text{m}^2$ was scanned in the x-z plane and an array of 100×80 Raman spectra was acquired with an integration time of 100 ms/spectrum. The measurements were performed with the green excitation laser and an air objective (NA = 0.9). Fig. 8a shows the unique Raman spectra of the two polymers (red and green) and the

characteristic Raman spectrum of cellulose (blue) and calcite (orange). The color-coded depth profile (Fig. 8b) shows that the two polymers are immiscible and form a sharp interface (red and green) in between them as well as with the paper beneath (blue and yellow).

The two examples show that confocal Raman imaging can be used to identify various coating layers on paper in a nondestructive way.

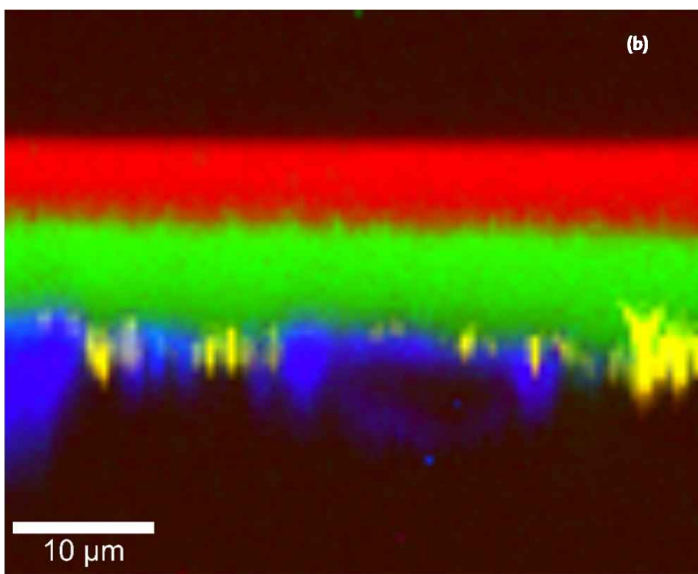
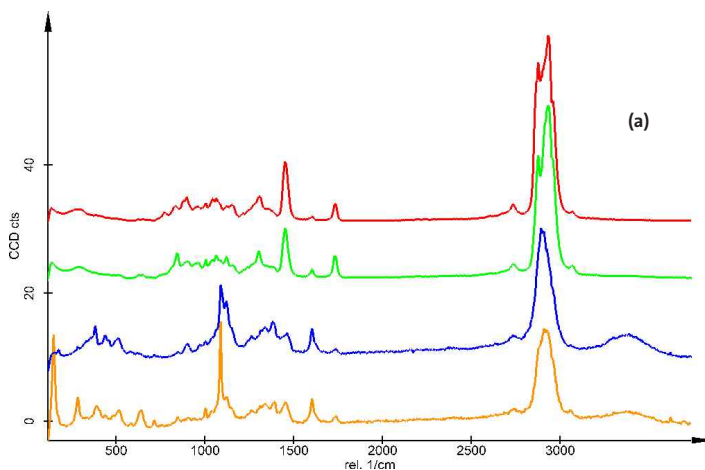


Fig. 8: Confocal Raman depth scan through a paper sticker. Raman spectra calculated from the spectral array (a) and color-coded Raman image of depth profile showing the two polymeric layers (red and green) applied on paper (yellow and blue). These two polymers form a strong interface, without penetrating into one another. Image area $50 \times 40 \mu\text{m}^2$, 100×80 pixels, integration time: 100 ms/spectrum.

Writing and Printing on Paper

“Who signed first? – And with which pen?”

Two common questions in forensic document forging investigation processes. Confocal Raman imaging can provide evidence of the use of various ballpoint pen marks on paper and the order in which these inks (pastes) were applied to the paper. Fig. 9a shows a video image recorded at the intersection of two different ballpoint pen marks. Paste 1 was applied on the right side of the video image and paste 2 on the left side. The possibility of an overlap of these two pastes cannot be excluded, however this is not evident from the video image alone. The area marked with

the red frame ($50 \times 50 \mu\text{m}^2$) was scanned in Raman spectral imaging mode by recording an array of 128×128 complete Raman spectra with an integration time of 100 ms/spectrum. From the array of spectra, three different Raman spectra were calculated. At some surface areas only luminescence could be detected (not shown as a spectrum), whereas other areas showed the unique Raman spectra presented in Fig. 9b. These two spectra show only very small differences of which some are highlighted with arrows in the figure. In the color-coded Raman image presented in Fig. 9c, blue denotes the luminescent areas while the distribution of the two ballpoint-pastes are represented in red and green. An area

where both pens can be seen is clearly visible. To prove the order in which these ballpoint pens were applied to the paper, a depth scan (x-z scan) along the black line in the video image (Fig. 9a) was performed. An array of 128×128 complete Raman spectra was acquired over $90 \mu\text{m}$ in the x-direction and $50 \mu\text{m}$ in the z-direction with an integration time of 100 ms/spectrum. The distribution along the depth profile of the two ballpoint pens pastes is shown in Fig. 9d, using the same color-code as for Fig. 9c. This depth profile clearly shows that the red marked paste was applied on top of the green marked paste, thus showing the order in which these pastes were applied to the paper.

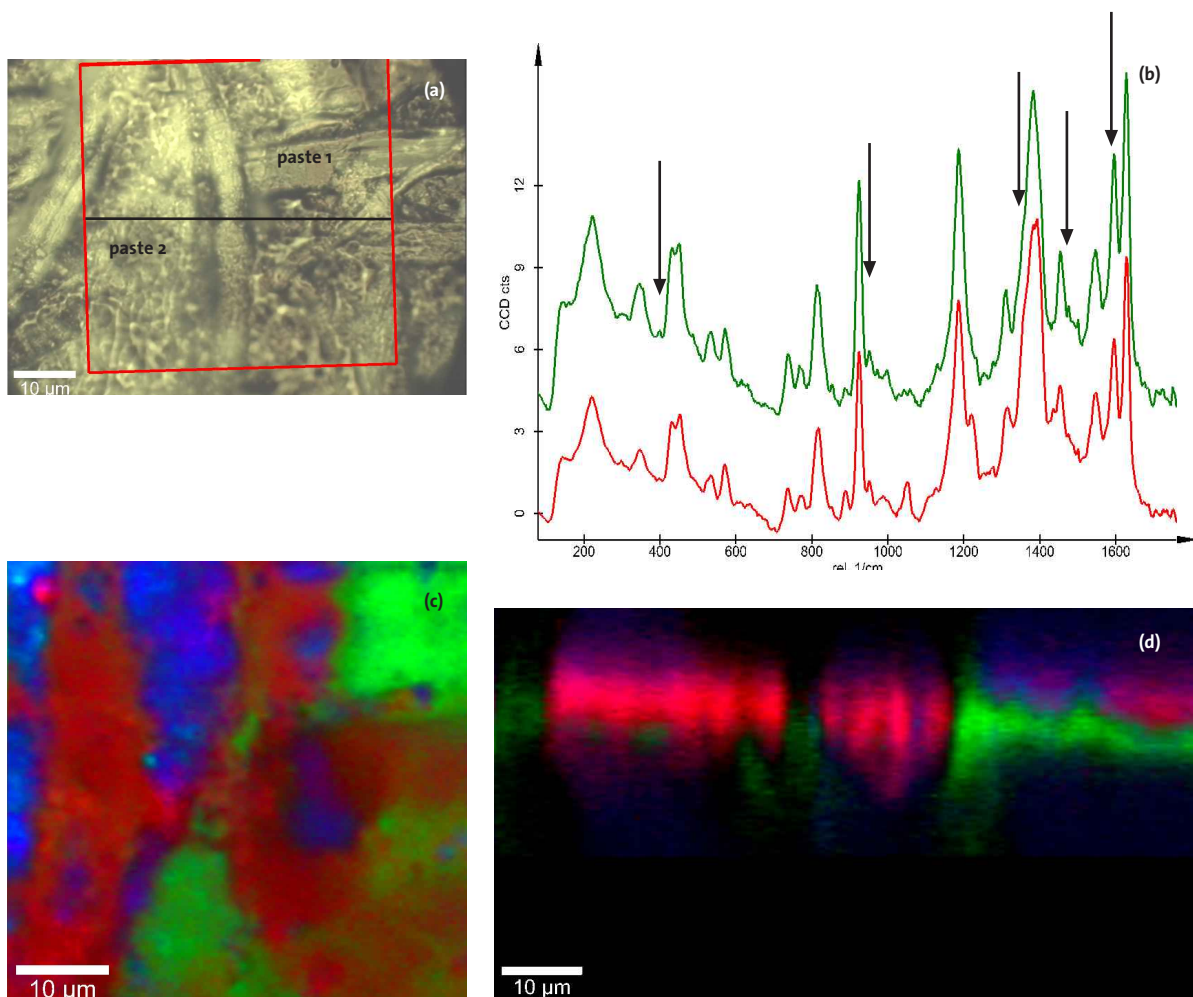


Fig. 9: Confocal Raman imaging of ballpoint writing on paper. Video image (a), evaluated Raman spectra (b), color-coded Raman image recorded from the paper surface, image area $50 \times 50 \mu\text{m}^2$, 128×128 pixels, integration time: 100 ms/spectrum (c), and color-coded depth profile, image area $90 \times 50 \mu\text{m}^2$, 128×128 pixels, integration time: 100 ms/spectrum (d). The ballpoint writing is shown in red and green in the images.

In the following examples a combined printing and ballpoint mark on paper is analyzed to show that by using Raman imaging it is possible to distinguish printer ink from ballpoint pen ink. These experiments require the analysis of large sample areas in the range of several millimeters and therefore the alpha500 R microscope equipped with a green laser and a 50x air objective (NA = 0.5) was used. In a first measurement the chemical composition of the printer ink distributed on the paper was examined. A sample area of 3x2 mm² was imaged in Raman spectral

imaging mode by acquiring an array of 150x150 Raman spectra with an integration time of 160 ms/spectrum. From this array three different spectra were calculated as shown in red and yellow color in Fig. 10a, whereas the third spectrum (not presented) showed strong fluorescence represented as green spots in Fig. 10b. The red spectrum is characteristic for the coated printer paper, whereas the yellow spectrum corresponds to the printing ink used to produce a yellow printed line as shown in the color-coded Raman image in Fig. 10b. Additionally, in the printer ink, strongly

fluorescent particles (represented in green in Fig. 10b) could be detected, which are distributed randomly over the printed line. In a second experiment, a ballpoint pen line was drawn across the border between the printed line and plain paper. A large area scan of 0.8x1.3 mm² was performed over the border between the paper, printed line and ballpoint pen writing. The distribution of paper, printed line and ballpoint pen mark is shown in Fig. 10c. The ink of the ballpoint pen (blue spectrum in Fig. 10a and blue color in Fig. 10c) shows significant spectral differences compared to the ink used in the printer. The measurements presented in this section show that confocal Raman imaging can contribute to the analysis of forensic material, providing information regarding printing material used and the order in which they were applied.

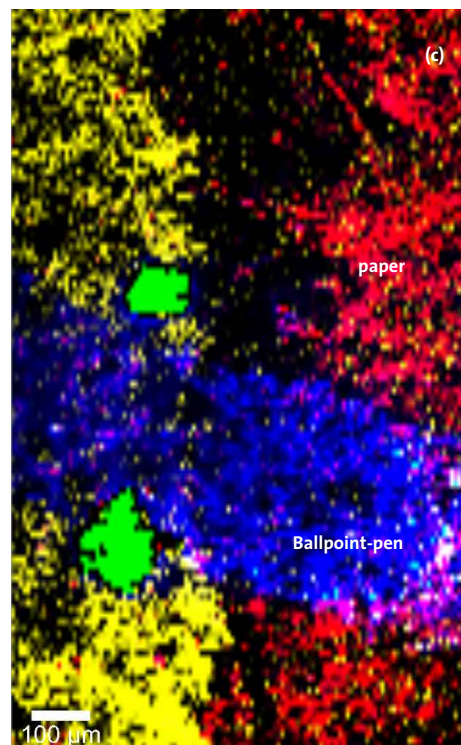
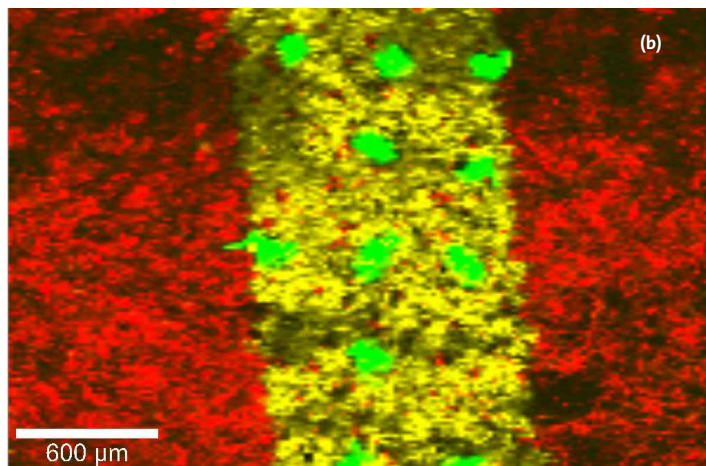
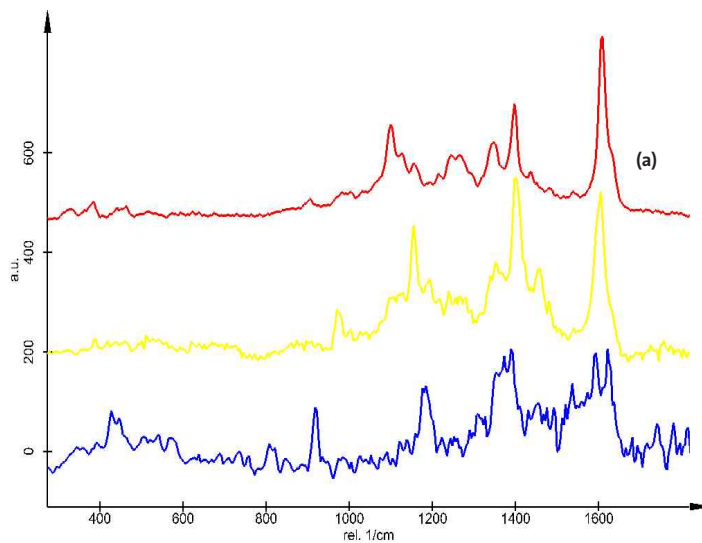


Fig. 10: Confocal Raman imaging of printing and ballpoint writing on paper: evaluated Raman spectra of paper (red), printer ink (yellow) and ballpoint ink (blue) (a), color-coded Raman image recorded from the paper surface after printing, image area 3x2 mm², 150x150 pixels, integration time: 160 ms/spectrum (b), and color-coded Raman image after printing and writing, image area 0.8x1.3 mm², 128x128 pixels, integration time: 160 ms/spectrum (c).

Summary

Confocal Raman microscopy provides information on the orientation of cellulose fibers resulting from the first step of paper production. In addition, several chemical residues from circulating water or wood extractives on cellulose fibers can be identified unambiguously. The roughness of

papers with various finishes can furthermore be determined on the nanometer scale using AFM.

The distribution of coating components such as calcite, starch, and polymeric material on cellulose fibers can also be identified using confocal Raman imaging. Finally, coating layers as well as the order in which printing

and writing were applied can be described in a non-destructive manner, without laborious sample preparation.

Confocal Raman imaging combined with high resolution AFM can thus contribute to a more detailed understanding of the micro- and nanostructures of paper as well as vital information in forensic applications.

References/Further Reading

1. Gierlinger N., Sapei L. and Paris O. (2008) Insights into the chemical compositions of *Equisetum hyemale* by high resolution Raman imaging. *Planta*, 227, 969-980.

2. Gierlinger N. and Schwamminger M. (2007) The potential of Raman microscopy and Raman imaging in plant research. *Spectroscopy*, 21, 69-89.

3. Characterization of Wood Cells and Cellulose Fibers, WITec Application Note, www.witec.de

4. Österberg M., Schmidt U. and Jääskeläinen A.-S. (2006) Combining confocal Raman spectroscopy and atomic force microscopy to study wood extractives on cellulose surfaces. *Colloids and Surfaces*, 291, 197-201.

5. Eronen P. and Österberg M. (2009) Effect of alkaline treatment on cellulose supramolecular structure studied with combined confocal Raman spectroscopy and atomic force microscopy. *Cellulose Journal*, 16:167 – 178,

6. WITec Project User Manual